Spin dynamics and magnetic ordering in the quasi-one-dimensional $S = \frac{1}{2}$ antiferromagnet $Na_2CuSO_4Cl_2$

M. Fujihala* and S. Mitsuda
Department of Physics, Faculty of Science, Tokyo University of Science, Shinjuku, Tokyo 162-8601, Japan

R. A. Mole and D. H. Yu
Australian Nuclear Science and Technology Organisation, Lucas Heights, New South Wales 2232, Australia

I. Watanabe
Meson Science Laboratory, Nishina Center, RIKEN, 2-1 Hirosawa, Wako, Saitama 351-0198, Japan

S. Yano
National Synchrotron Radiation Research Center, Neutron Group, Hsinchu 30077, Taiwan

T. Kuwai
Graduate School of Science and Engineering, University of Toyama, Toyama 930-8555, Japan

H. Sagayama
Institute of Materials Structure Science, High Energy Accelerator Research Organization, Tsukuba, Ibaraki 305-0801, Japan

T. Kouchi, H. Kamebuchi, and M. Tadokoro
Department of Chemistry, Faculty of Science, Tokyo University of Science, Shinjuku, Tokyo 162-8601, Japan

(Received 12 July 2019; revised manuscript received 10 December 2019; published 15 January 2020)

The $S = \frac{1}{2}$ quasi-one-dimensional antiferromagnet $K_2CuSO_4X_2$ (X = Cl, Br) exhibits peculiar Dzyaloshinskii-Moriya (DM) interactions that are uniform along its spin chains and antiparallel with respect to neighboring chains. This feature has received much attention recently because it leads to spin frustration, however, the spin dynamics around T_N and magnetic structure have not been reported. Here we report magnetic behaviors of $Na_2CuSO_4Cl_2$. The orthorhombic crystal structure of $Na_2CuSO_4Cl_2$, which is identical to $K_2CuSO_4X_2$, was verified. The results of the thermodynamic measurements suggest that this compound has moderately strong intra- and interchain interaction for investigation of the spin state around T_N. The inelastic neutron scattering and muon spin relaxation and rotation measurements reveal the presence of a two-spinon continuum, and below T_N, the long-range order develops. However, the obtained critical exponent is $\beta = 0.18$, which is not indicative of a three-dimensional magnetic system; instead, one-dimensional (1D) spin correlation likely affects the formation of magnetic ordering in $Na_2CuSO_4Cl_2$. There is a possibility that $Na_2CuSO_4Cl_2$ is a model compound for investigation of DM-induced frustration effects in a 1D quantum spin system.

DOI: 10.1103/PhysRevB.101.024410

I. INTRODUCTION

One-dimensional (1D) spin systems have received intense attention because they are expected to be promising candidates for novel quantum states. Intensive studies of 1D antiferromagnets have successfully captured some exotic quantum states, such as the Tomonaga-Luttinger spin-liquid state [1] and the Haldane state [2]. In real magnetic systems, any interchain coupling will induce magnetic ordering at finite temperatures. Therefore, to identify quantum phases, it is usually important to explore a model compound that contains a nearly ideal 1D spin chain. On the other hand, weak interchain interaction plays an important role in quasi-1D $S = \frac{1}{2}$ spin systems with uniform Dzyaloshinskii-Moriya (DM) interaction in realizing an exotic spin state [3,4]. Systems with such a feature have received much attention recently because they are expected to exhibit geometrical frustration. For a single spin chain, the effect of the DM interaction simply favors a helimagnetic spin arrangement, in which the spiral period is determined by the ratio of the magnitude of the DM interaction D to that of the intrachain exchange constant J, D/J [5]. However, helical correlations with opposing helicity are present in materials where interacting spin chains feature peculiar DM interactions that are uniform along the chain and antiparallel with respect to neighboring chains, thus resulting in unique spin frustration. Whether or not this frustration will affect magnetic ordering will depend on how D compares to interchain interaction J'.

*fujihara@nsmsmac4.ph.kagu.tus.ac.jp

TABLE I. Comparison of the exchange constants for $K_2CuSO_4X_2$ (X = Cl, Br) and $Na_2CuSO_4Cl_2$; the intrachain interactions J are obtained by magnetic susceptibility measurements [8]. The interchain interactions J' are estimated from the Néel temperature [8,13] and inelastic neutron scattering measurements [10].

	$K_2CuSO_4Cl_2$	$K_2CuSO_4Br_2$	$Na_2CuSO_4Cl_2$
J	3.2 K [8]	20.4 K [8]	14.3 K
J'	0.031 K [8]	0.034 K [8]	0.18 K
J' (INS)	0.45 K [10]	–	–

Some copper salts are known to be quasi-1D $S = \frac{1}{2}$ spin systems, hence enabling the experimental study of quantum magnetism [6,7]. The Cu^{2+} salts $K_2CuSO_4X_2$ (X = Cl, Br), which are 1D quantum spin systems with uniform DM interaction, exhibit magnetic properties due to their quantum spin chains [8–12]. Linear spin chains along the a axis are formed by the exchange interaction through the Cu-Cl(Br)-Cl(Br)-Cu path, which is much larger than the interchain interaction [8].

Based on their crystal structure, $K_2CuSO_4X_2$ feature substantial DM interactions that are aligned parallel to the b axis and in the same direction with a chain. However, the DM vector is aligned antiparallel between adjacent chains. The intrachain exchange interactions were estimated to be $J_{Cl} = 3.2$ K and $J_{Br} = 20.4$ K, and the interchain coupling constants $J'_{Cl} = 0.031$ K and $J'_{Br} = 0.034$ K were obtained for the chloride and bromide compounds, respectively (see Table I). Inelastic neutron scattering data of $K_2CuSO_4Br_2$ measured at 1.5 K show the presence of a two-spinon continuum along the chain. Both compounds exhibit long-range magnetic order below 0.1 K [8]. The spin state of $K_2CuSO_4X_2$ in the high-temperature region, which is a Tomonaga-Luttinger spin liquid state, has already been revealed by comprehensive experimental studies. However, the spin dynamics around T_N and magnetic structure have not been reported.

To understand the DM-induced frustration effects in quasi-1D quantum spin systems, systematic study of the spin dynamics and magnetic structure of $K_2CuSO_4X_2$ and family compounds of it are useful, because the magnetic ground state is controlled by the magnitude of J' and D. Here we report magnetic behaviors of $Na_2CuSO_4Cl_2$, which we successfully synthesized as large crystals weighing more than 10 g. We investigate the magnetism in this compound through magnetic susceptibility, heat capacity, inelastic neutron scattering (INS), and muon-spin rotation and relaxation (μSR) measurements.

II. EXPERIMENTAL DETAILS

Large single crystals of $Na_2CuSO_4Cl_2$ were successfully grown by using a low-temperature molten-salt reaction process. High-purity $CuCl_2$ and Na_2SO_4 powders were mixed with the molar ratio of 1 : 1 and vacuum sealed into a quartz tube. The mixture was heated at 470 °C for two days and then slowly cooled. The crystal structure of the ground single crystal was examined and determined by synchrotron x-ray diffraction (XRD). Synchrotron powder XRD data were collected using an imaging plate diffractometer installed at BL-8B of the Photon Factory. An incident synchrotron x-ray energy of 18.0 keV (0.68892 Å) was selected. The Rietveld refinement was conducted using the RIETAN-FP program [14]. Diffraction data for single crystal were measured on Brüker D8 QUEST x-ray diffractometer with CMOS PHOTON III detector and by using a monochromatized Mo-$K\alpha$ radiation through a multilayered mirror from an enclosed x-ray tube source apparatus. Data reduction, structure solution and refinement, and all the necessary computational data processes were performed using the APEXIII [15], SAINT [16], and SHELXTL-2014 programs [17], and for absorption using SADABS [18]. Magnetic susceptibility measurements were performed using a commercial superconducting quantum interference device magnetometer (MPMS; Quantum Design). The specific heat was measured between 0.2 and 30 K using a PPMS (physical property measurement system; Quantum Design). The INS experiments were performed using the cold-neutron time-of-flight spectrometer PELICAN at the OPAL reactor at ANSTO [19]. The instrument was aligned for incident energies $E_i = 3.68$ and 14.7 meV. The sample was held on an aluminum plate and cooled down by a top loading closed-cycle refrigerator; data was collected at 1.5 and 30 K. The sample was corrected for background scattering from an empty sample holder and normalized to the scattering from a vanadium standard. Data was processed using a combination of the freely available LAMP and HORACE software [20,21]. The μSR experiment was carried out using a spin-polarized single-pulsed surface-muon (μ^+) beam at the RIKEN-RAL Muon Facility at Rutherford Appleton Laboratory in the United Kingdom. A ^{3}He cryostat was used for temperature control.

III. RESULTS AND DISCUSSION

The orthorhombic crystal structure of $Na_2CuSO_4Cl_2$, which is identical to $K_2CuSO_4X_2$ was verified. Therefore, $Na_2CuSO_4Cl_2$ is expected to exhibit peculiar DM interactions that are uniform along its spin chains and antiparallel with respect to neighboring chains. The lattice parameters are refined to be $a = 7.0324(2)$ Å, $b = 5.6054(1)$ Å, $c = 16.0344(4)$ Å, and the positions of the individual atoms are also determined as presented in Table II (full details are given in the Supplemental Material as CIF files [22]). As shown in Fig. 1(a), the nearest- and the next-nearest-neighbor Cu^{2+} ions are located along the b axis. Apical bonds mediate the exchange paths through the Cu-Cl-Cu bonds since the Jahn-Teller elongation occurs along the b axis [see Figs. 1(b) and 1(c)]. Therefore, the magnetic coupling along the b axis is likely weak. The linear spin chains are also formed by the intrachain exchange interaction J_{Na} through the Cu-Cl-Cl-Cu path in $Na_2CuSO_4Cl_2$. The bonding angles Cu-Cl-Cl are refined as 148.26(7)° and 130.75(7)°. The $3d_{x^2-y^2}$ orbital lies within the CuO_2Cl_2 plaquette. And the plaquettes in a chain are in the same plane. Therefore, the exchange interaction through the Cu-Cl-Cl-Cu exchange path is expected to be the antiferromagnetic interaction, in fact, our experimental results support it (discussed below). The Cu-Cu bond lengths along the chain and b axis are 7.035 and 3.559 Å for $Na_2CuSO_4Cl_2$, 7.732 and 3.784 Å for $K_2CuSO_4Cl_2$, respectively. Thus, the

TABLE II. Structure information of $Na_2CuSO_4Cl_2$ refined from single-crystal XRD data measured at 303 K.

	Chemical formula		$Na_2CuSO_4Cl_2$	
	Cell setting		orthorhombic	
	Space group		*Pnma*	
	a (Å)		7.0324(2)	
	b (Å)		5.6054(1)	
	c (Å)		16.0344(4)	
Atom	*x*	*y*	*z*	Site
Na1	0.36348(18)	0.75000	0.39357(9)	4c
Na2	0.6002(2)	0.25000	0.21587(11)	4c
Cu	0.86444(5)	0.75000	0.46576(2)	4c
S	0.84910(10)	0.75000	0.30373(5)	4c
O1	0.6892(3)	0.75000	0.36511(13)	4c
O2	1.0211(3)	0.75000	0.35958(12)	4c
O3	0.8463(2)	0.5359(3)	0.25212(10)	8d
Cl1	0.64081(11)	0.75000	0.56421(5)	4c
Cl2	1.12300(10)	0.75000	0.54778(5)	4c

intra- and interchain interactions of $Na_2CuSO_4Cl_2$ are expected to be stronger than that of $K_2CuSO_4Cl_2$.

In Fig. 2(a) the magnetic susceptibility is shown as measured at 0.1 T. No anomaly indicative of long-range order is observed down to 1.9 K. A broad peak is observed at approximately 10 K, thus suggesting the presence of a 1D antiferromagnetic correlation. The data is fitted to the Bonner-Fisher expression with an antiferromagnetic interaction $J_{Na} = 14.3(1)$ K [23].

Evidence of the 1D antiferromagnetic correlation and transition is given by the specific heat. As shown in Fig. 2(b), a broad anomaly is also verified around 10 K, indicating the presence of a 1D antiferromagnetic correlation. The magnetic specific heat for linear-chain system with $J_{Na} = 14.3$ K is calculated by the quantum Monte Carlo method using the

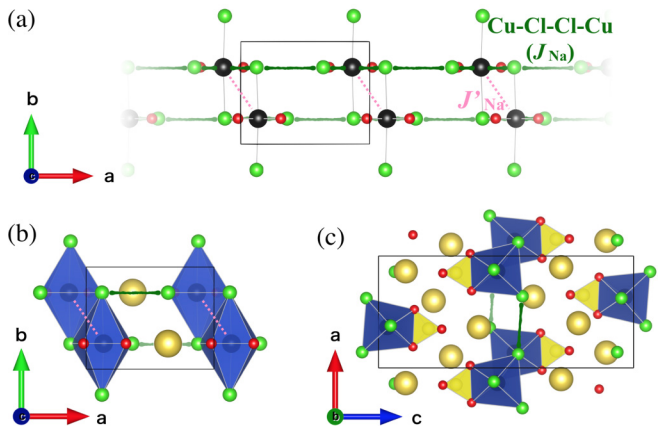

FIG. 1. (a) The crystal structure of $Na_2CuSO_4Cl_2$. The Cu^{2+} ions (black) displayed with nearby oxygen (red) and chlorine ions (green). The linear spin chain of $Na_2CuSO_4Cl_2$, which forms due to the intrachain exchange interaction through the Cu-Cl-Cl-Cu path (green solid line). The pink dashed lines indicate the interchain exchange interaction. (b) and (c) The Cu^{2+} ions are six coordinated in a distorted octahedral geometry. The Na^+ ions (yellow balls) displayed with SO_4 ions (yellow tetrahedra).

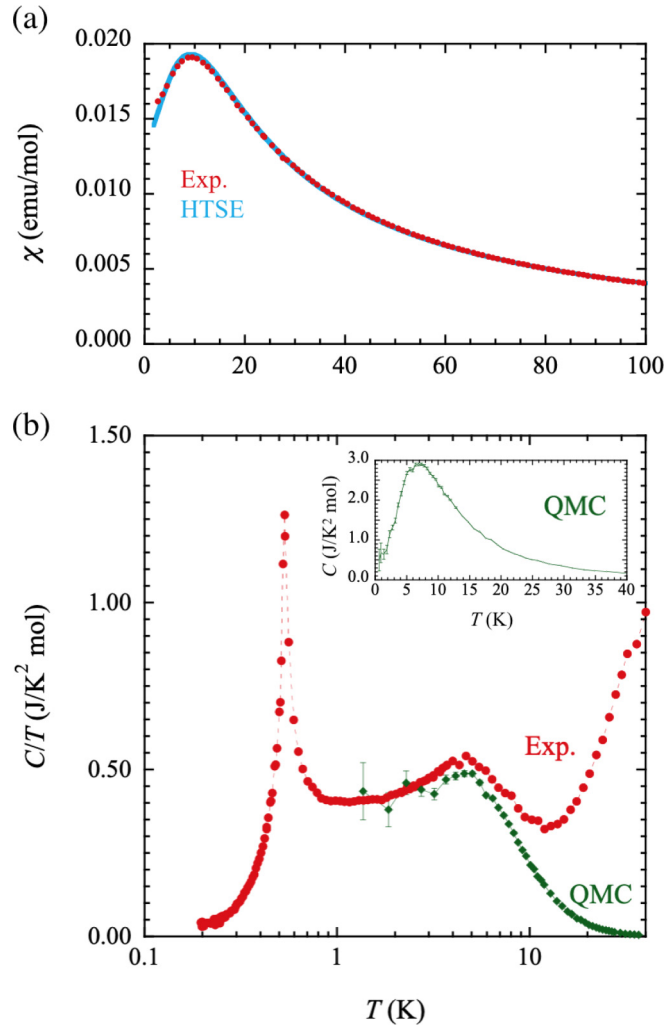

FIG. 2. (a) Temperature dependence of the magnetic susceptibility χ (open red circles) of $Na_2CuSO_4Cl_2$ measured at 0.1 T. The blue solid line is a fit to the Bonner-Fisher curve for $S = \frac{1}{2}$ linear chain Heisenberg antiferromagnet. (b) The temperature dependence of the total specific heat (filled red circles) divided by temperature (C/T) for zero magnetic field. The filled green squares are the theoretical data of the linear spin chain model, which was computed by the quantum Monte Carlo method. Inset shows a linear-linear plot of the theoretical data.

ALPS package [24]. We cannot assume the nonmagnetic contribution to the experimental data, however, the calculated result is in good agreement with the experimental data in the lower-temperature region. The specific heat curve shows a pronounced λ-shaped peak at $T_N = 0.54$ K, which signifies a second-order phase transition. We estimated the interchain interaction $J'_{Na} = 0.18$ K of $Na_2CuSO_4Cl_2$ from the Néel temperature [13]. Very recently, the magnitude of J'_{Cl} for $K_2CuSO_4Cl_2$ obtained by INS experiment was reported to be 0.45 K [10]. This is about 15 times greater than that estimated from T_N (see Table I). Further study is requested to clarify the appropriate magnitude of J'_{Na}.

The ratio of T_N to the intrachain interaction J is 0.038 in $Na_2CuSO_4Cl_2$, which is close to that of $K_2CuSO_4Cl_2$ (T_N/J are 0.025 and 0.005 for $K_2CuSO_4Cl_2$ and $K_2CuSO_4Br_2$,

respectively). The magnitude of $J'_{\rm Br}$ in $K_2CuSO_4Br_2$ is much smaller than that of $J_{\rm Br}$; therefore, the competition between the interchain exchange and uniform DM interaction would not affect the spin arrangement. The $T_{\rm N}$ of $K_2CuSO_4X_2$ are reported about 0.1 K, therefore, a dilution refrigerator must be employed in the experiment below $T_{\rm N}$. There is a possibility that this is the reason why the magnetic structure of $K_2CuSO_4X_2$ have not been revealed. On the other hand, evidence that $Na_2CuSO_4Cl_2$ has uniform DM interaction have not been obtained. Further study is needed to judge whether this compound is a model compound for investigation of DM-induced frustration effects in a 1D quantum spin system or not.

To confirm the antiferromagnetic interaction through Cu-Cl-Cl-Cu bond along the a axis dominates in this system and the observation of a gapless low-energy spin excitation, we performed an INS measurement. As shown in Fig. 3(a), the spin excitations show no variation in position with h. This dispersionless behavior is a signature characteristic of excitations in a 1D antiferromagnet. The intensity at $h = -1.5$ shows a clear variation with a minimum at $l = 0$ and it is symmetrical about this point. This is possibly an artifact of the measurement, for example absorption. Measurements taken at 1.5 K show gapless and continuous magnetic excitation only along the a^* axis [see Figs. 3(b) and 3(c)]. The continuum edges rise up from the Brillouin zone centers in the chain direction, $h = -0.5$, -1.5, and -2.5. In addition, the observed lower energy boundary of the continuum is consistent with the theoretical line for the 1D spin-$\frac{1}{2}$ Heisenberg antiferromagnet given by Eq. (1):

$$(\pi J_{\rm Na}/2)|\sin(2\pi h)|, \tag{1}$$

thus indicating that the velocity of the spin excitations of $Na_2CuSO_4Cl_2$ is appropriate for the 1D spin-$\frac{1}{2}$ Heisenberg antiferromagnet [25]. A continuum is reflected in the dynamical structure factor probed by INS, and the constant-energy (constant-E) cuts can be described by the approximate, semiempirical Müller ansatz (MA) equation [26,27]. As shown in Fig. 4(a), the result of fitting the MA equation to the data is reasonably good. The intrachain interaction refined as $J_{\rm Na} = 14.2(3)$ [see Fig. 4(b)], which is close to that obtained from a magnetic susceptibility measurement. Therefore, we conclude that the linear spin chains along the a axis are formed by the exchange interaction $J_{\rm Na} = 14.3(1)$ K through the Cu-Cl-Cl-Cu path. Measurements taken at 30 K show that the faintly remaining intensity is broad in both momentum and energy, however, it exists in the area inside the upper energy boundary of the continuum [see Figs. 5(a) and 5(b)]. As discussed below, this indicates that a spinon excitation persists up to at least this temperature.

Zero-field (ZF)-μSR measurements on a powder sample provide evidence for static magnetic ordering in $Na_2CuSO_4Cl_2$. The muon spin precession frequencies are clearly observed and disappear at the temperature corresponding to the peak in the specific heat curve, as shown in Fig. 6(a). The spectra for $T > 0.54$ K are best fit by

$$a(t) = a_0 \exp(-\lambda_{\rm H.T.} t) G^{\rm KT}(t, \Delta) + a_{\rm BG}, \tag{2}$$

where a_0 is the intrinsic asymmetry $a_0 = 13.5$, $a_{\rm BG}$ is the constant background $a_{\rm BG} = 6.1$, $\lambda_{\rm H.T.}$ is the relaxation rate,

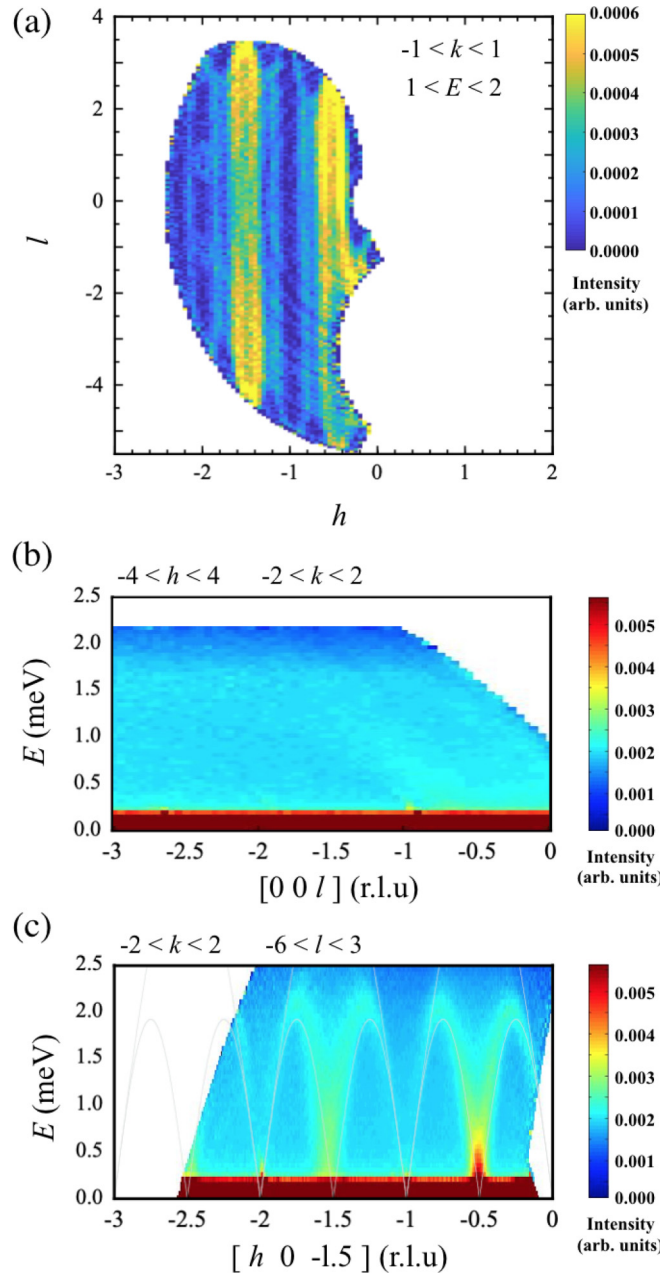

FIG. 3. (a) Contour map at constant-E cut and neutron scattering intensity at $T = 1.5$ K with incident neutron energy of 3.68 meV. The energy window was from $E = 1$ to 2 meV, and the scattering was integrated over $-1 \leqslant k \leqslant 1$. INS spectra (b) along the c^* axis and (c) along the a^* axis of $Na_2CuSO_4Cl_2$ measured at 1.5 K with incident neutron energy of 3.68 meV. The intensities were integrated over h from -4 to 4, k from 2 to 2 and k from -2 to 2, l from 6 to 3. The superimposed gray solid lines indicate the lower and upper energy boundaries of the continuum given by $(\pi J_{\rm Na}/2)|\sin(\pi h)|$ and $\pi J_{\rm Na}|\sin(\pi h/2)|$ [25].

and $G^{\rm KT}(t, \Delta)$ is the Kubo-Toyabe function. The field distribution is $\Delta/\gamma_\mu = 2.2$ G, which is typical for a nuclear dipolar field of Cl nuclei, suggesting that most positive muons stop in the vicinity of the Cl^- ions [28]. For powder samples, long-range magnetic ordering is characterized by asymmetry oscillation followed by a constant one-third polarization at

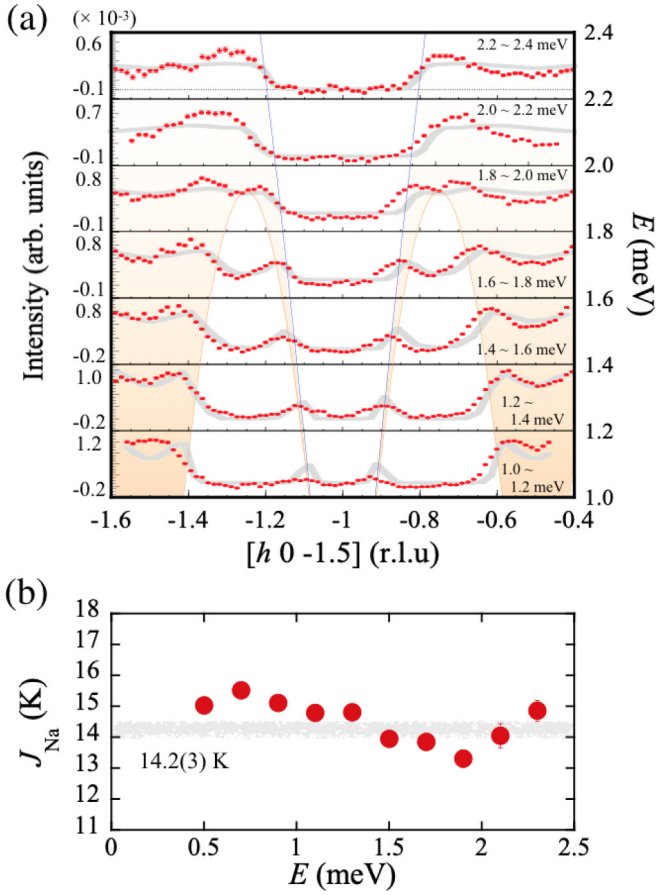

FIG. 4. (a) Constant-E cuts of the measured scattering intensity of Fig. 3(c). The superimposed orange and blue solid lines indicate the lower and upper energy boundaries of the continuum. The intensity in each panel is integrated within the energy range shown in the upper right corner. The gray thick lines are the fits using the approximate, semiempirical Müller ansatz expression (see Eq. (4) in Ref. [26]). (b) The intrachain interaction J_{Na} refined by fitting cuts at different E.

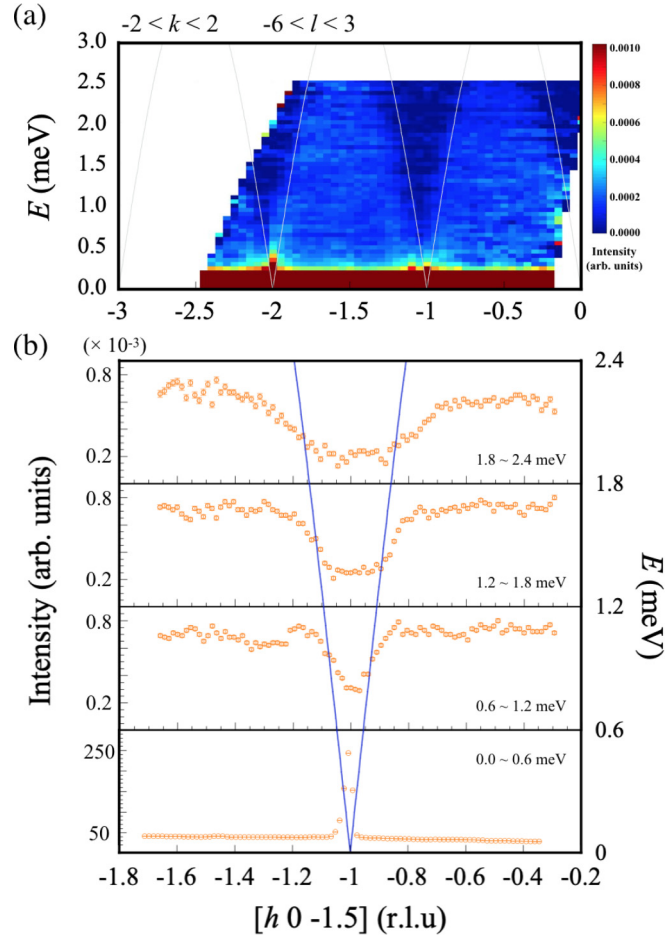

FIG. 5. (a) INS spectrum along the a^* axis of $Na_2CuSO_4Cl_2$ measured at 30 K with incident neutron energy of 3.68 meV. (b) Constant-E cuts of the measured scattering intensity of (a). The superimposed blue solid lines indicate the upper energy boundaries of the continuum. The intensity in each panel is integrated within the energy range shown in the lower or upper right corner.

long times, the so-called one-third tail. As shown in Fig. 6(b), the tail of the ZF spectrum at the lowest temperature (0.34 K) increase, which is a strong evidence for long-range magnetic ordering in $Na_2CuSO_4Cl_2$. Moreover, longitudinal field (LF) decoupling behavior is typical for static magnetically ordered systems [Fig. 6(c)]. For $T \leqslant 0.54$ K, the spectra are well fitted by three distinct frequencies corresponding to three stopping sites for muons. The ZF-μSR asymmetry function for three-muon stopping sites is given by

$$\begin{aligned} a(t) = a_1[&f_1 \exp(-\lambda_1 t)\cos(\gamma_\mu B_1 t) \\ &+ f_2 \exp(-\lambda_2 t)\cos(\gamma_\mu B_2 t) \\ &+ (1 - f_1 - f_2)\exp(-\lambda_3 t)\cos(\gamma_\mu B_3 t)] \\ &+ a_2 \exp(-\lambda_{\mathrm{L}} t) + a_{\mathrm{BG}}, \end{aligned} \tag{3}$$

where a_1 and a_2 are the intrinsic asymmetries $a_1 = 9.0$ and $a_2 = 4.5$, respectively, λ_i ($i = 1$ to 3) and λ_{L} are the relaxation rates of the transverse and longitudinal component, respectively, B_i are internal magnetic fields. In $Na_2CuSO_4Cl_2$l, three possible stopping sites exist for the positive muons: one near the SO_4 and two near the two Cl ions. The f_1 and f_2 represent the muon fractions stopped at the different muon sites which result from two Cl sites. Adding a third component with 11% leads to a perfect agreement with the oscillation data. The component represents the muons stop near the SO_4 ions. The a_2 is one-third of the relaxing asymmetry, and the nonprecessing (longitudinal) component. The temperature dependence of the relaxation rates increased rapidly when the temperature approached $T_{\mathrm{N}} = 0.54$ K, thus implying a critical slowing toward T_{N} [see Fig. 6(d)]. The temperature dependence of the internal magnetic fields B_i decrease with increasing temperature and vanished at T_{N}, as shown in Fig. 6(e). Analyzing the data with the power law,

$$B_i = B_i(0)[1 - (T/T_{\mathrm{N}})]^{\beta} \tag{4}$$

yields the critical exponent $\beta = 0.18$, and the internal magnetic fields $B_1(0) = 280.64$ G, $B_2(0) = 174.29$ G, and $B_3(0) = 69.19$ G. The value of β is different from the critical exponent expected for a 3D magnetic system ($\beta = 0.36$). Such behavior is often observed in low-dimensional systems [29].

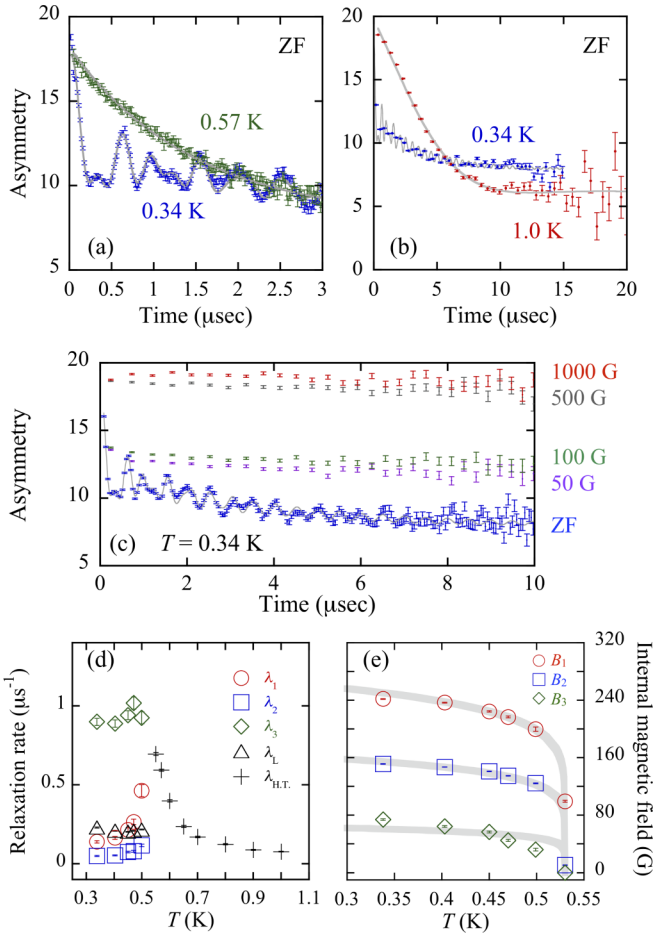

FIG. 6. (a) ZF-μSR spectra measured on a powder sample of $Na_2CuSO_4Cl_2$ at representative temperatures. The thick lines behind the data points are curves fitted with a fixed constant background of $a_{BG} = 6.1$ (see text). (b) ZF-μSR spectra measured at 0.34 and 1.0 K, showing the fitted time window up to 20 μs. (c) μSR spectra measured at 0.34 K under ZF and representative external fields. (d) Temperature dependence of the muon spin relaxation rates. (e) Temperature dependence of the internal magnetic fields, and the gray solid lines are power-law fit curves.

To discuss the development of short-range correlations at temperatures above that of the 14.3(1) K (J_{Na}), we investigated the spin dynamics by performing LF-μSR measurements on a single crystal of $Na_2CuSO_4Cl_2$ with the incident beam parallel to the a axis. As mentioned, the field distribution of the nuclear dipoles is $\Delta/\gamma_\mu = 2.2$ G, therefore we applied a 50G LF to decouple the contribution of nuclear dipolar fields. The relaxations are very weak, as shown in Fig. 7(a), but a distinct increase in the relaxation rate is observed at higher temperatures. The spectra can be described by the exponential relaxation function

$$a(t) = a_r \exp(-\lambda t) + a_{nr}, \tag{5}$$

where the relaxing asymmetry a_r is fixed and a_{nr} is a non-relaxing component. In a conventional 3D antiferromagnet, paramagnetic moments critically slow down as T_N is approached, which results in an increase in the spin relaxation rate λ with decreasing temperature. Although critical slowing

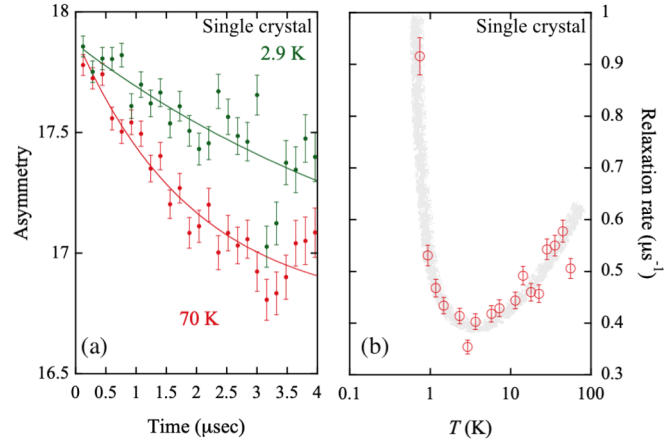

FIG. 7. (a) Weak LF-μSR spectra measured on a single crystal of $Na_2CuSO_4Cl_2$ at 2.9 and 70 K in a longitudinal external magnetic field of 50 G. The thick lines behind the data points are curves fitted to the data by Eq. (5). (b) Temperature dependence of the muon spin relaxation rate λ. The gray solid line is guide to the eye.

down is certainly observed near T_N, the λ increases with the increasing temperature, which continues up to at least 70 K [Fig. 7(b)]. We suggest that this is caused by diffusive spin transport in a 1D spin chain. The μSR method is not selective for the wave vector of the spin excitations. Therefore, at low-temperature (but above T_N), the spin relaxation can be described by a sum of the Brillouin zone centers and $q = 0$ components. In that case, the temperature dependence of λ is known to be quadratic [30]. In the quasi-1D $S = \frac{1}{2}$ spin systems, the thermal conductivity due to spinons was observed at higher temperature than that of J [31]. Therefore, λ increases with increasing temperature even at higher temperatures.

IV. CONCLUSIONS

In summary, we presented the Cu^{2+} salt $Na_2CuSO_4Cl_2$ as a quasi-1D quantum spin system with conjectured uniform DM interaction. The μSR and INS studies demonstrated that the quantum state of a 1D spin-$\frac{1}{2}$ Heisenberg antiferromagnet, which was previously revealed for the related compounds $K_2CuSO_4X_2$ (X = Cl, Br), is present in $Na_2CuSO_4Cl_2$. Our work also shows that long-range ordering is present in $Na_2CuSO_4Cl_2$. Moreover, unconventional value of the critical exponent β and diffusive spin transport above T_N are observed. We suggest that 1D spin correlation influences the formation of magnetic ordering in $Na_2CuSO_4Cl_2$. Further study is in progress to determine its magnetic structure. Moreover, ESR experiment is required to obtain evidence that this compound has uniform DM interaction. Since the transition in $Na_2CuSO_4Cl_2$ occurs in a readily accessible range of temperatures, future study of DM-induced frustration effects in a 1D quantum spin system are expected to be facilitated.

ACKNOWLEDGMENTS

Synchrotron powder XRD measurements were performed with the approval of the Photon Factory Program Advisory

Committee (Proposal No. 2016G030). The μ SR experiment is supported by the RIKEN Nishina Center for Accelerator-Based Science. This study is supported by the Grant- in-Aid for Scientific Research (No. 17K14344) from MEXT, Japan.

[1] I. A. Zaliznyak, Nat. Mater. **4**, 273 (2005).
[2] I. Affleck, J. Phys.: Condens. Matter **1**, 3047 (1989).
[3] M. Kargarian, R. Jafari, and A. Langari, Phys. Rev. A **79**, 042319 (2009).
[4] I. Garate and I. Affleck, Phys. Rev. B **81**, 144419 (2010).
[5] I. Dzyaloshinskii, J. Phys. Chem. Solids **4**, 241 (1958).
[6] H. Tanaka, K. Takatsu, W. Shiramura, and T. Ono, J. Phys. Soc. Jpn. **65**, 1945 (1996).
[7] K. Yu. Povarov, A. I. Smirnov, O. A. Starykh, S. V. Petrov, and A. Ya. Shapiro, Phys. Rev. Lett. **107**, 037204 (2011).
[8] M. Hälg, W. E. A. Lorenz, K. Yu. Povarov, M. Månsson, Y. Skourski, and A. Zheludev, Phys. Rev. B **90**, 174413 (2014).
[9] A. I. Smirnov, T. A. Soldatov, K. Yu. Povarov, M. Hälg, W. E. A. Lorenz, and A. Zheludev, Phys. Rev. B **92**, 134417 (2015).
[10] D. Blosser, N. Kestin, K. Yu. Povarov, R. Bewley, E. Coira, T. Giamarchi, and A. Zheludev, Phys. Rev. B **96**, 134406 (2017).
[11] W. Jin and O. A. Starykh, Phys. Rev. B **95**, 214404 (2017).
[12] T. A. Soldatov, A. I. Smirnov, K. Yu. Povarov, M. Hälg, W. E. A. Lorenz, and A. Zheludev, Phys. Rev. B **98**, 144440 (2018).
[13] C. Yasuda, S. Todo, K. Hukushima, F. Alet, M. Keller, M. Troyer, and H. Takayama, Phys. Rev. Lett. **94**, 217201 (2005).
[14] F. Izumi and K. Momma, Solid State Phenom. **130**, 15 (2007).
[15] Bruker APEX3, V2016. 1-0, Bruker AXS Inc., Madison, WI, USA, 2015.
[16] Bruker SAINT, V8. 37a, Bruker AXS Inc., Madison, WI, USA, 2012.
[17] G. M. Sheldrick, Acta Crystallogr. Sect. C **71**, 3 (2015).
[18] G. M. Sheldrick, SADABS, University of Göttingen: Göttingen, Germany, 2007.
[19] D. Yu, R. Mole, T. Noakes, S. Kennedy, and R. Robinson, J. Phys. Soc. Jpn. **82**, SA027 (2013).
[20] D. Richard, M. Ferrand, and G. J. Kearley, J. Neutron Res. **4**, 33 (1996).
[21] R. A. Ewings, A. Buts, M. D. Le, J. van Duijn, I. Bustinduy, and T. G. Perring, Nucl. Instrum. Methods Phys. Res. A **834**, 132 (2016).
[22] See Supplemental Material at http://link.aps.org/supplemental/10.1103/PhysRevB.101.024410 for CIF files from x-ray structure refinement.
[23] J. C. Bonner and M. E. Fisher, Phys. Rev. **135**, A640 (1964).
[24] A. F. Albuquerque, F. Alet, P. Corboz, P. Dayal, A. Feiguin, S. Fuchs, L. Gamper, E. Gull, S. Gürtler, A. Honecker, R. Igarashi, M. Körner, A. Kozhevnikov, A. Läuchli, S. R. Manmana, M. Matsumoto, I. P. McCulloch, F. Michel, R. M. Noack, G. Pawłowski, L. Pollet, T. Pruschke, U. Schollwöck, S. Todo, S. Trebst, M. Troyer, P. Werner, and S. Wessel, J. Magn. Magn. Mater. **310**, 1187 (2007).
[25] B. Lake, D. A. Tennant, C. D. Frost, and S. E. Nagler, Nat. Mater. **4**, 329 (2005).
[26] G. Müller, H. Thomas, H. Beck, and J. C. Bonner, Phys. Rev. B **24**, 1429 (1981).
[27] I. A. Zaliznyak, H. Woo, T. G. Perring, C. L. Broholm, C. D. Frost, and H. Takagi, Phys. Rev. Lett. **93**, 087202 (2004).
[28] M. Fujihala, X. G. Zheng, H. Morodomi, T. Kawae, and I. Watanabe, Phys. Rev. B **87**, 144425 (2013).
[29] M. Isobe, H. Okabe, E. Takayama-Muromachi, A. Koda, S. Takeshita, M. Hiraishi, M. Miyazaki, R. Kadono, Y. Miyake, and J. Akimitsu, J. Phys.: Conf. Ser. **400**, 032028 (2012).
[30] F. L. Pratt, S. J. Blundell, T. Lancaster, C. Baines, and S. Takagi, Phys. Rev. Lett. **96**, 247203 (2006).
[31] T. Kawamata, M. Uesaka, M. Sato, K. Naruse, K. Kudo, N. Kobayashi, and Y. Koike, J. Phys. Soc. Jpn. **83**, 054601 (2014).